Supplementary Material (ESI) for Chemical Communications

Enhanced Stability of Blue-Green Light-Emitting Electrochemical Cells Based on a Cationic Iridium Complex with 2-(1-Phenyl-1*H*-Pyrazol-3-yl)pyridine as the Ancillary Ligand

Lei He, Lian Duan,* Juan Qiao, Deqiang Zhang, Liduo Wang and Yong Qiu*
Key Lab of Organic Optoelectronics and Molecular Engineering of Ministry of Education,
Department of Chemistry, Tsinghua University, Beijing 100084 (P. R. China)

General Experiments. All reactants and solvents, unless otherwise stated, were purchased from commercial sources and used as received. ^{1}H-NMR and ^{13}C-NMR spectra were recorded on a JOEL JNM-ECA600 NMR spectrometer with $Si(CH_3)_4$ as the internal standard. Mass spectrometry was performed with a Thermo ELECTRON CORPORATION Finnigan LTQ mass spectrometer. Elemental analysis was determined on an Elementar Vario EL CHN elemental analyzer. Absorption spectra were recorded with a UV-vis spectrophotometer (Agilent 8453). PL spectra were recorded with a fluorospectrophotometer (Jobin Yvon, FluoroMax-3). The PL transient lifetimes were measured on a transient spectrofluorimeter (Edinburgh Instruments, FLSP920) with a time-correlated single-photon counting technique. The PLQY of the complex (excited at 390 nm) was measured in degassed CH_3CN solutions with quinine sulfate ($\Phi_p = 0.545$ in 1 M H_2SO_4) as the standard.[1] The PLQYs in thin films were measured with an integrating sphere on a fluorospectrophotometer (Jobin Yvon, FluoroMax-3) according to a reported procedure.[2] Cyclic voltammetry was performed on a Princeton Applied Research potentiostat/galvanostat model 283 voltammetric analyzer in CH_3CN solutions (10^{-3} M) at a scan rate of 100 mV/s, with a Pt plate as the working electrode, a Ag wire as the pseudo-reference electrode and a Pt wire as the counter electrode. The supporting electrolyte was tetrabutylammonium hexafluorophosphate (0.1 M) and ferrocene was selected as the internal standard. The solutions were degassed with argon before measurements.

Synthesis of complex 1

Synthesis of 2-(1-phenyl-1H-pyrazol-3-yl)pyridine (phpzpy). The reactant 2-(1*H*-pyrazol-3-yl) pyridine was purchased from Alfa Aesar. Copper(I) iodide (0.19 g, 1 mmol) and 1,10-phenanthroline (0.39 g, 2 mmol) were dissolved in dimethylformamide (20 ml). The solution was heated at 80 ℃ under Ar atmosphere and turned black immediately. After 2 h, the solution was cooled to room temperature. To the solution, iodobenzene (0.85 ml, 7.6 mmol), 2-(1*H*-pyrazol-3-yl)pyridine (0.71 g, 5 mmol) and cesium carbonate (3.26 g, 10 mmol) were added under Ar atmosphere. The mixture was refluxed at 110 ℃ for 48 h under Ar atmosphere. The solvent was removed under vacuum and the residue was extracted with dichloromethane (100 ml). The product was obtained by column chromatography on silica gel (200-300 mesh) with petroleum ether/ethyl acetate (15:1) as the eluent, yielding a wax-like solid (0.81 g, 3.7 mmol). Yield: 74%. ^{1}H-NMR (chloroform-d_6, 600 MHz, δ[ppm]): 8.655(d, J=4.86Hz, 1H), 8.13 (d, J=8.3 Hz, 1H), 7.99 (d, J=2.8 Hz, 1H), 7.79 (d, J=7.6 Hz, 2H), 7.75 (t, J=7.6 Hz, 1H), 7.47 (t, J=7.6 Hz, 2H), 7.31 (t, J=7.6 Hz, 1H), 7.24 (m, 1H), 7.14 (d, J=2.8 Hz, 1H). ESI-MS [m/z]: 222.12 $[M+H]^+$.

The by-product 2-(1-phenyl-1*H*-pyrazol-5-yl)pyridine was obtained as a viscous liquid (0.18 g, 0.8 mmol). Yield: 16%. ^{1}H-NMR (chloroform-*d*$_6$, 600 MHz, δ[ppm]): 8.59 (d, J=4.8 Hz, 1H), 7.75 (d, J=2.1 Hz, 1H), 7.59 (t, J=7.9 Hz, 1H), 7.38-7.29 (m, 5H), 7.22-7.17 (m, 1H), 7.15 (d, J=8.2 Hz, 1H), 6.80 (d, J=2.1 Hz, 1H). ESI-MS [m/z]: 222.16 $[M+H]^+$.

Synthesis of [Ir(ppy)$_2$(phpzpy)]PF$_6$ (complex 1). The dichloro-bridged diiridium complex $[Ir(ppy)_2Cl]_2$ (0.7 g, 0.65 mmol) and phpzpy (0.28 g, 1.26 mmol) were suspended in ethane-1,2-diol (40 mL). The mixture was refluxed at 140 ℃ for 15 h under Ar atmosphere, to result in a clear yellow solution. The solution was cooled to room temperature and diluted with deionized water (100 ml). To the solution, an aqueous solution of NH_4PF_6 (2.0 g in 10 mL of deionized water) was slowly added under stirring, to result in a yellow suspension. The suspension was then filtered and the resultant precipitate was washed with deionized water and dried under vacuum at 70 ℃ for 5 h. The crude product was purified by column chromatography on silica gel (200-300 mesh) with CH_2Cl_2/acetone (50:1) as the eluent, to yield a bright-yellow solid (0.81 g, 0.93 mmol). Yield: 72%. The ^{1}H-NMR and ^{13}C-NMR spectra of complex 1 are presented in Figure S1-S3. ^{1}H-NMR (acetone-*d*$_6$, 600 MHz, δ[ppm]): 8.54 (d, J=8.2 Hz, 1H), 8.25-8.19 (m, 2H), 8.14 (t, J=8.6 Hz, 3H), 8.01 (t, J=7.9 Hz, 1H), 7.95 (t, J=7.9 Hz, 1H), 7.90 (d, J=5.5 Hz, 1H), 7.84 (d, J=5.5 Hz, 1H), 7.77 (d, J=8.2 Hz, 1H), 7.67 (d, J=2.8 Hz, 1H), 7.54-7.47 (m, 2H), 7.30 (t, J=6.5 Hz, 1H), 7.21 (t, J=6.5 Hz, 1H), 7.16-7.11 (m, 1H), 7.01-6.94 (m, 5H), 6.84 (t, J=7.2 Hz, 1H), 6.64 (t, J=7.6 Hz, 1H), 6.39 (t, J=7.6 Hz, 1H), 6.14 (d, J=7.6 Hz, 1H), 5.76 (d, J=7.6 Hz, 1H). ^{13}C-NMR (DMSO-d_6, 600 MHz, δ[ppm]): 107.91, 120.18, 120.44, 121.57, 122.97, 123.90, 124.01, 124.75, 124.86, 125.39, 125.98, 127.35, 129.00, 129.59, 130.21, 130.76, 130.85, 131.51, 137.16, 138.52, 139.17, 139.21, 140.34, 144.05, 144.34, 147.51, 148.18, 149.66, 150.49, 151.77, 154.19, 166.73, 167.99. ESI-MS [m/z]: 722.25 [M-PF$_6$]$^+$. Anal. Found: C, 49.84; H, 3.32; N, 8.05. Anal. Calcd. for $C_{36}H_{27}F_6N_5PIr$: C, 49.88; H, 3.14; N, 8.08.

Synthesis of complex 2

Complex 2 was synthesized and characterized by the reported procedure.[3]

Crystal structure determination. Single crystal of complex 1 was grown from slow evaporation of an acetone/methanol solution. The room temperature single-crystal X-ray experiments were performed on a Bruker APEX CCD deffractometer equipped with graphite monochromatized Mo Kα radiation. Direct phase determination yielded the positions of all non-hydrogen atoms which were subjected to anisotropic refinement. All hydrogen atoms were generated theoretically and rode on their parent atoms in the final refinement. All computations were performed using the SHELXTL NT ver. 5.10 program.[4]

Theoretical calculations. Density functional theory (DFT) and time-dependent DFT (TD-DFT) at the B3LYP level were adopted for calculations on the ground and excited electronic states of the complex.[5-6] The geometry of the complex was optimized based on the single crystal structure. “Double-ξ” quality basis sets were employed for C, H and N (6-31G**) and the Ir (LANL2DZ). An effective core potential (ECP) replaces the inner core electrons of Ir leaving the outer core $(5s)^2(5p)^6$

electrons and the $(5d)^6$ valence electrons of Ir(III). The geometry of the singlet ground state (S_0) was fully optimized with a C1 symmetry constraint. All calculations were carried on with Gaussian 03 software package using a spin-restricted formalism.[7]

Fabrication and characterization of LEC devices. ITO substrates with a sheet resistance of 15 Ω/□ were sufficiently cleaned in detergent and then in deionized water. The ITO substrates were treated with UV-zone before use. The PEDOT: PSS layer was spin coated onto the ITO substrate in air and baked at 200 ℃ for 10 minutes. The PEDOT: PSS-coated substrate was transferred into a nitrogen-filled glove box, where the emissive layer was spin coated on top of PEDOT:PSS from CH_3CN solutions. The film was baked at 75 ℃ for 40 minutes and the substrate was then transferred into a metal-evaporating chamber connected to the glove box. The aluminum cathode was evaporated at an evaporating rate of 8-10 Å/s. The resultant device was transferred back to the glove box where the device was characterized with Keithley 4200 semiconductor characterization systems. The EL spectrum was collected with a Photo Research PR705 spectrophotometer in ambient conditions.

Figures and Tables

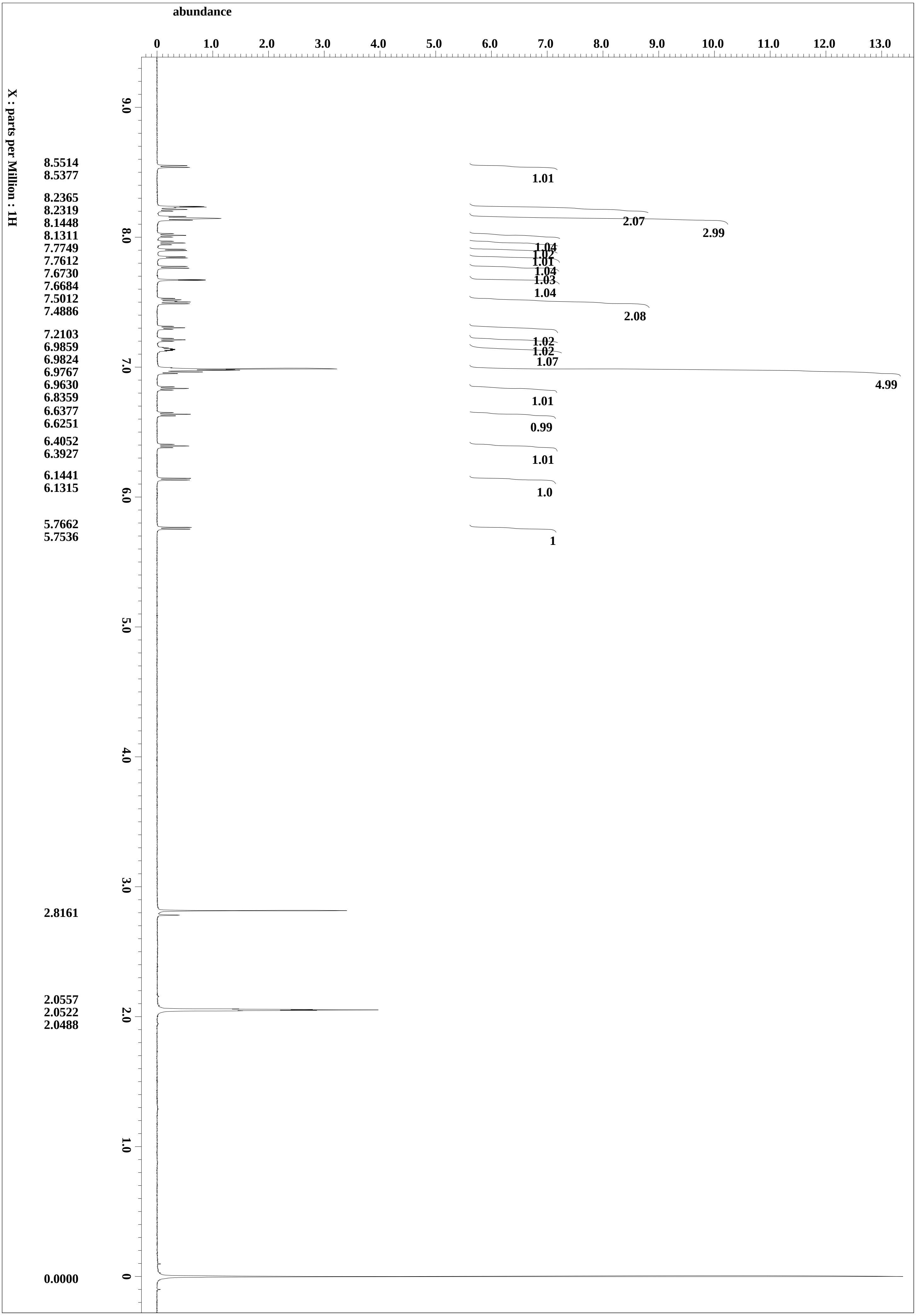

Figure S1. ^{1}H-NMR (600 M) spectrum of complex **1** in d_6-acetone.

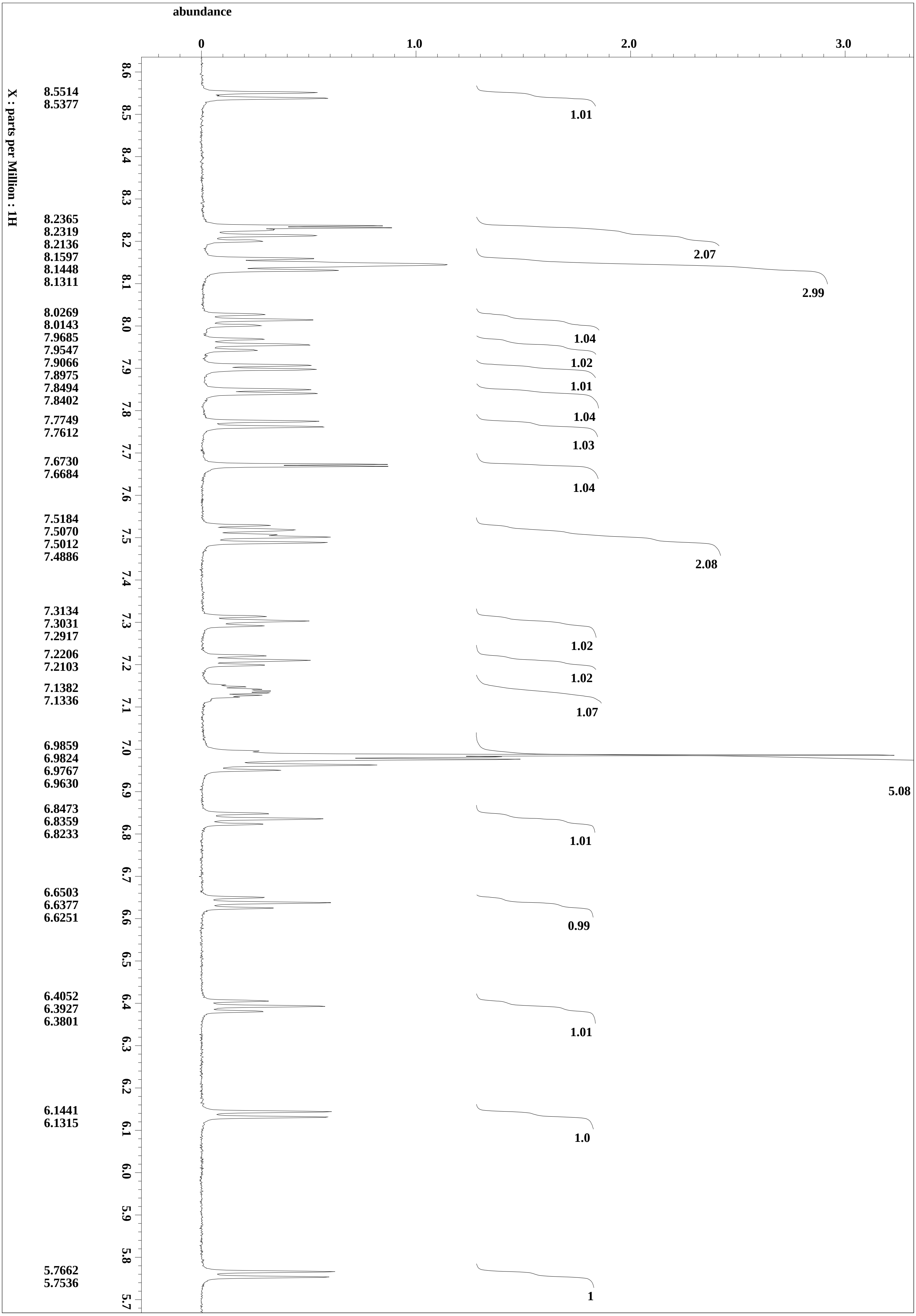

Figure S2. Zoomed ^{1}H-NMR (600 M) spectrum of complex 1 in d_6-acetone.

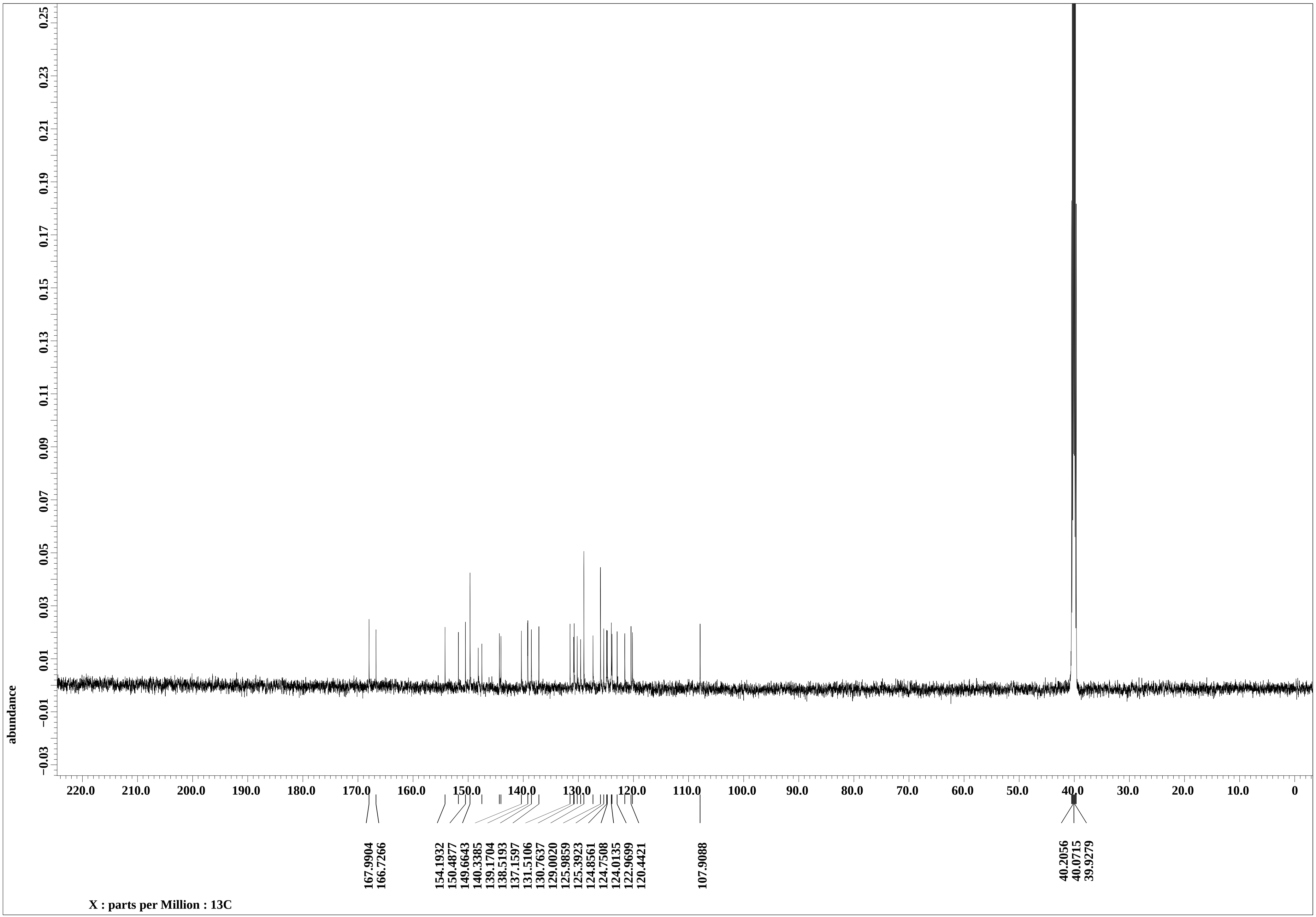

Figure S3 (a). ^{13}C-NMR (600 M) spectrum of complex 1 in d_6-DMSO.

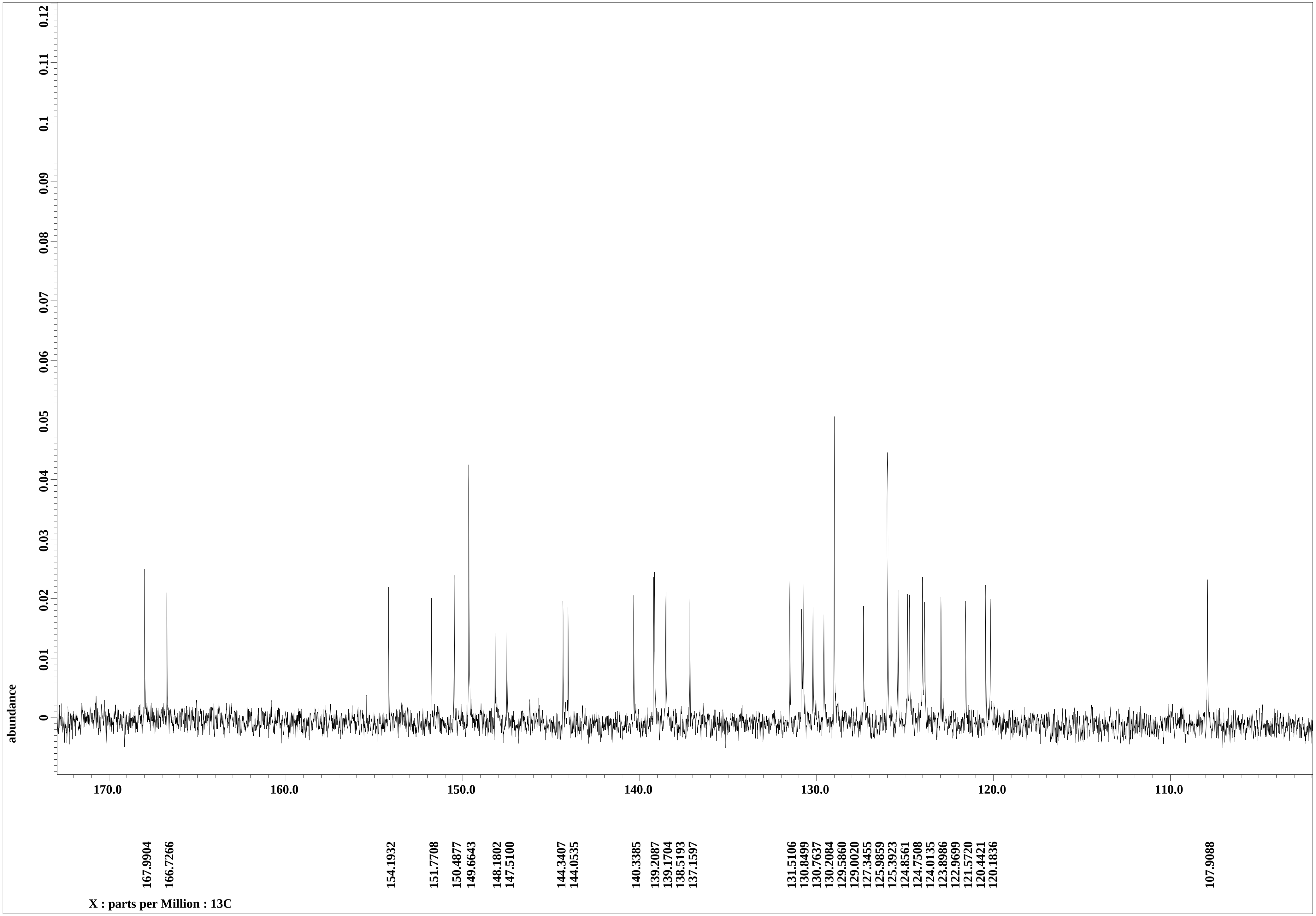

Figure S3 (b). Zoomed ^{13}C-NMR (600 M) spectrum of complex 1 in d_6-DMSO.

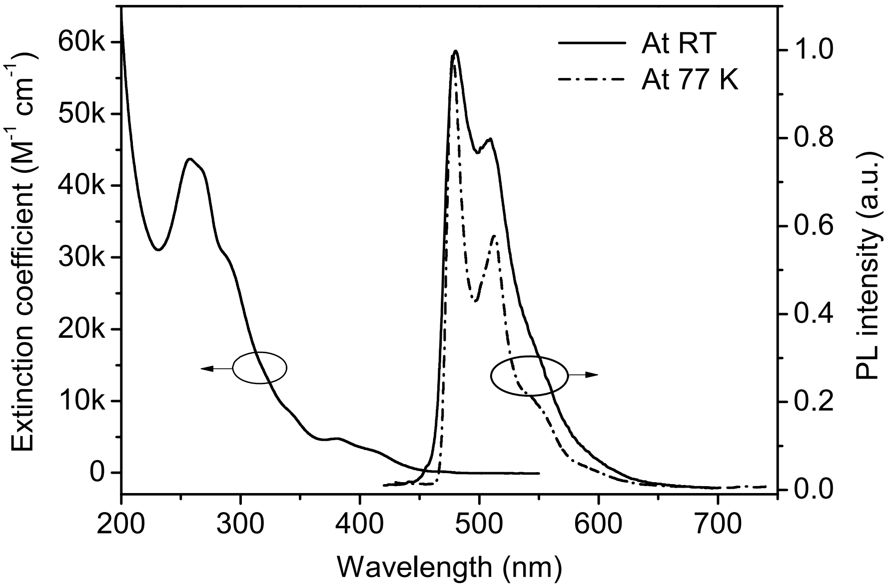

Figure S4. Absorption and PL spectra of complex 1 in CH_3CN solution at room temperature (RT) and at 77 K.

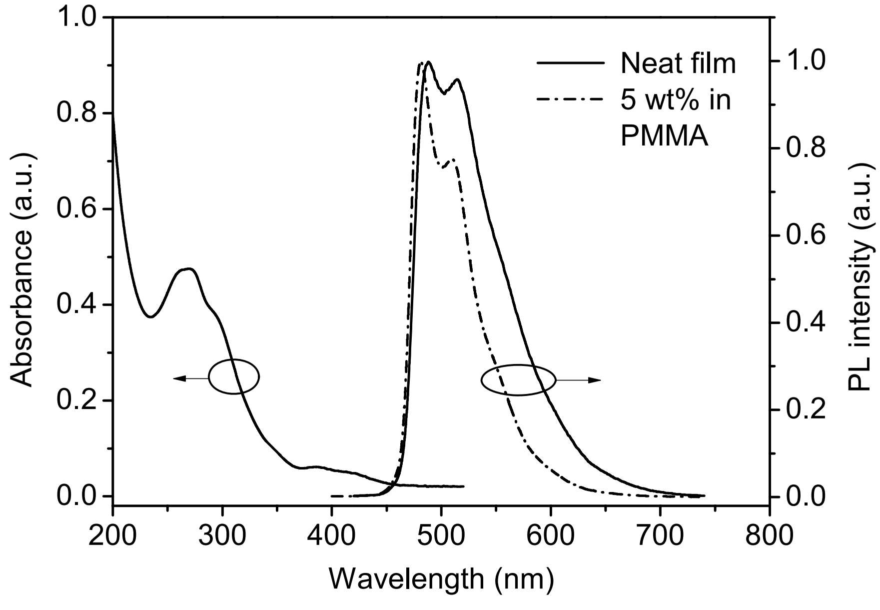

Figure S5. Absorption and PL spectra of complex 1 in neat film and in 5wt% doped PMMA film

Table S1. Photophysical and electrochemical characteristics of complex 1 in CH_3CN solutions.

Absorption λ [nm] (ε[×10^4 M^{-1} cm^{-1}]) [a]	PL at room temperature [b]			PL at 77 K [c]		Electrochemical Data [d]	
	λ [nm]	$Φ_{em}$	τ [μs]	λ [nm]	τ [μs]	$E_{ox}^{1/2}$ [V]	$E_{red}^{1/2}$ [V]
256 (4.36), 385 (0.47), 411 (0.31)	480, 509	0.03	0.18	478, 512	3.46	0.86	-2.15

[a] In 1×10^{-5} M CH_3CN solution. [b] In degassed 1×10^{-5} M CH_3CN solution. [c] In a frozen CH_3CN glass. [d] In degassed 10^{-3} M CH_3CN solution. Potentials were recorded versus Fc^+/Fc.

Table S2. Photophysical characteristics of complex 1 in thin films.

PL in Neat film [a]			PL in 5 wt % doped PMMA film [a]		
λ [nm]	$Φ_{em}$	τ [μs] [b]	λ [nm]	$Φ_{em}$	τ [μs]
486, 513	0.07	0.18 (74%), 0.43 (26%)	481, 510	0.84	3.02

[a] Films deposited on quartz substrates with a thickness of about 100 nm. [b] The PL exhibits a multi-exponential decay.

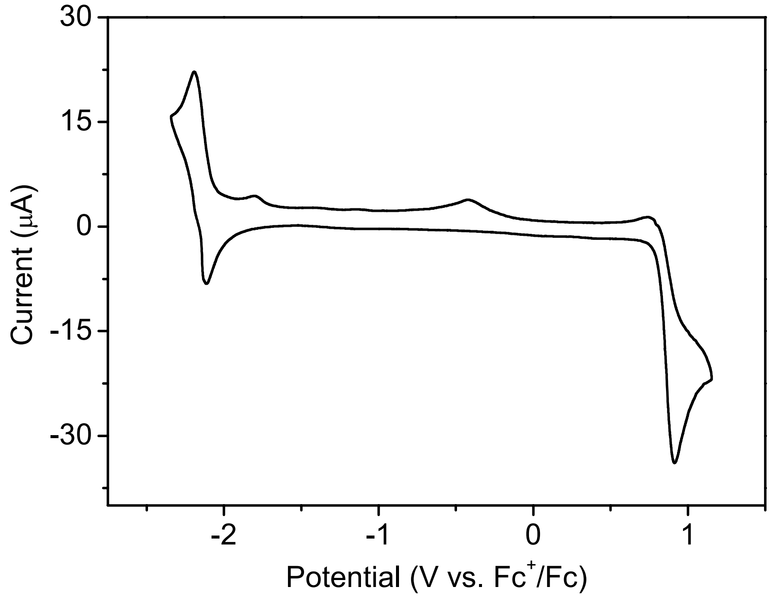

Figure S6. Cyclic voltammogram of complex 1 in CH_3CN solution (10^{-3} M).

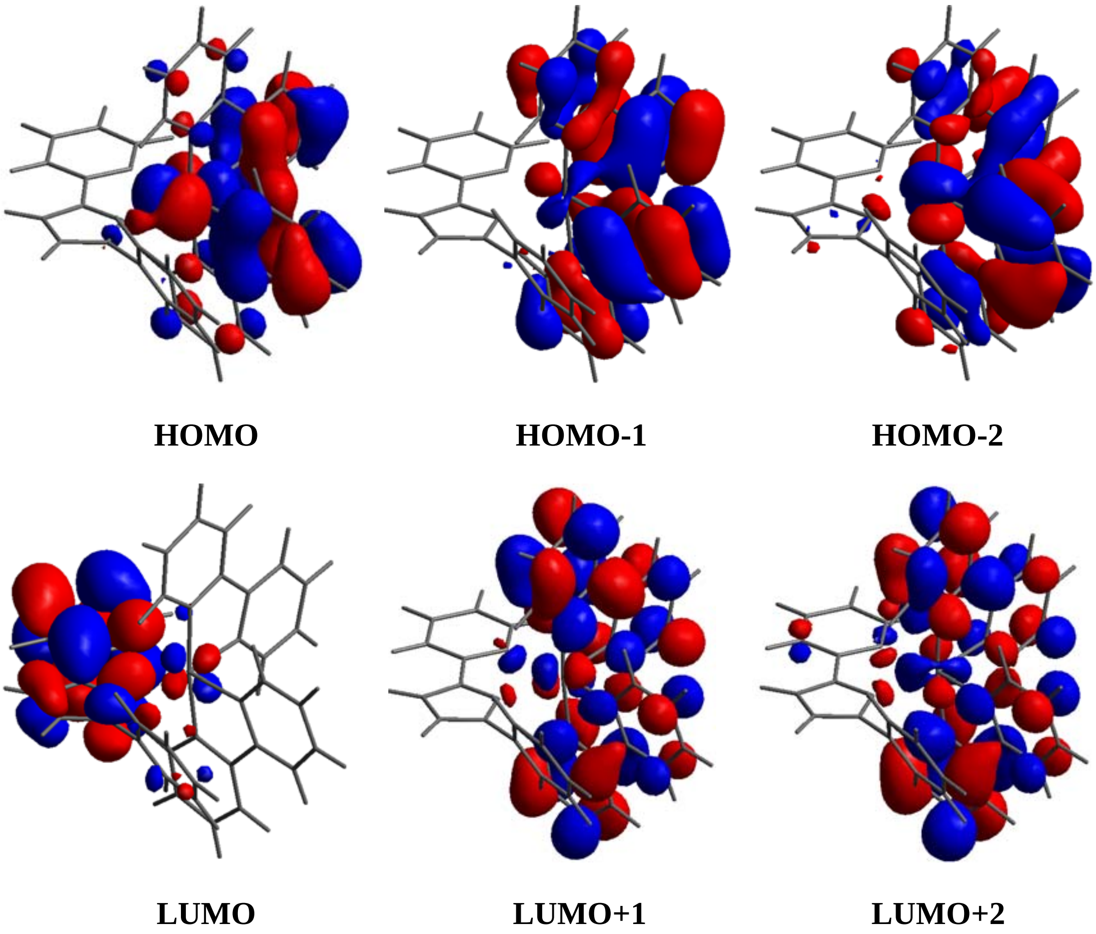

Figure S7. Molecular surfaces of complex 1. All the MO surfaces correspond to an isocontour value of |Ψ| = 0.025.

Table S3. Selected triplet states of complex 1 calculated from TDDFT approach.

States	E [eV] [a]	Dominant Excitations [b]	Nature
T_1	2.60	H → L (97%)	dπ(Ir)-π(ppy) → π*(phpzpy)
T_2	2.70	H → L+1 (63%), H-1 → L+2 (19%)	dπ(Ir)-π(ppy) → π*(ppy)
T_3	2.77	H → L+2 (44%), H-1 → L+1 (36%), H-2 → L+2 (10%)	dπ(Ir)-π(ppy) → π*(ppy)
T_4	3.04	H-4 → L (37%), H-2 → L (29%), H-6 → L (18%), H-8 → L (12%)	dπ(Ir)-π(ppy) → π*(phpzpy) π(phpzpy) → π*(phpzpy)

[a] Calculated excitation energies. [b] H and L denote HOMO and LUMO, respectively; data in parentheses are the contributions of excitations.

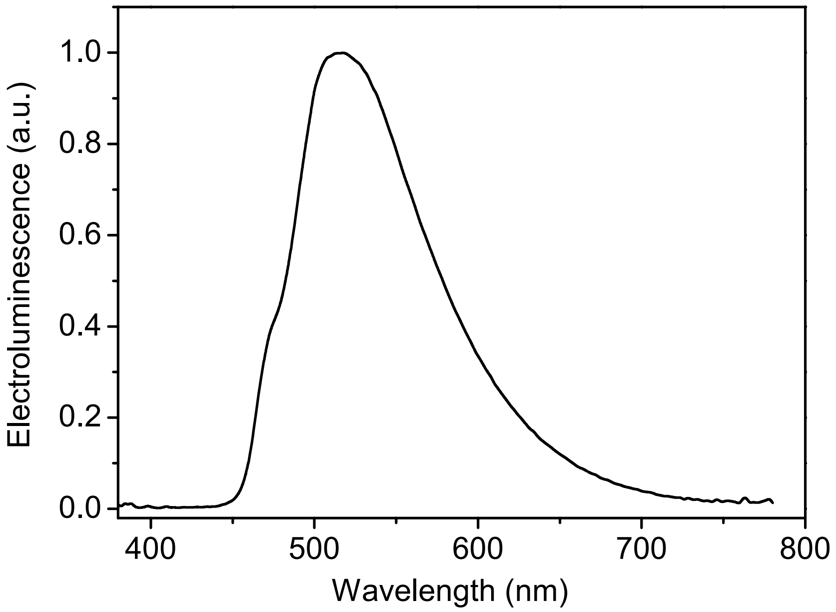

Figure S8. EL spectrum of the LEC based on complex 2.

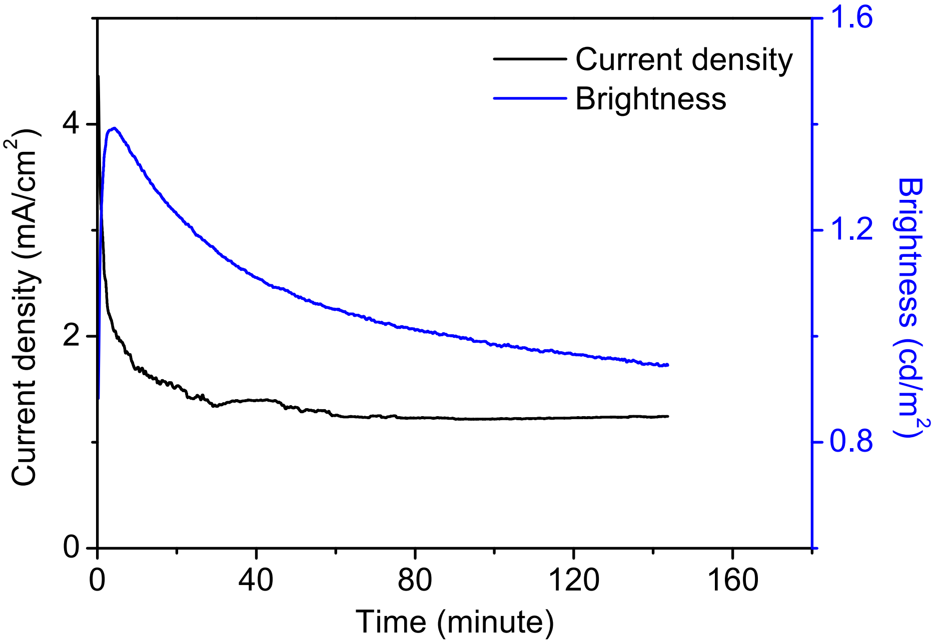

Figure S9. Current-density and brightness versus time at 3 V for the LEC based on complex 2.

Table S4. Electrical characteristics of LECs at 3 V.

Complex	t_{max} [min] [a]	B_{max} [cd/m^2]	$\eta_{c,\ max}$ [cd/A] [b]	EQE_{max} [c]	$t_{1/2}$ [min] [c]	E_{tot} [mJ] [d]	EL λ [nm]	CIE (x, y)
1	325	37	8.7	3.4%	950	52	486,512	(0.26,0.48)
2	3.8	1.4	0.1	0.03%	300	0.03	514,474	(0.30,0.54)

[a] Time required to reach the peak brightness. [b] The peak current efficiency. [c] The peak external quantum efficiency. [c] Time for the brightness to decay to half of the maximum. [d] Total emitted energy.

References

[1] W. H. Melhuish, *J. Phys. Chem.* **1961**, 65, 229.

[2] L. O. Pålsson, A. P. Monkman, *Adv. Mater.* **2002**, 14, 757.

[3] L. He, L. Duan, J. Qiao, R. Wang, P. Wei, L. D. Wang, Y. Qiu, *Adv.Funct. Mater.* 2008, 18, 2123.

[4] Bruker. (1997) SHELXTL. Structure Determination Programs, Version 5.10, Bruker AXS Inc., 6300 Enterprise Lane, Madison, WI 53719-1173, USA.

[5] A. D. Becke, *J. Chem. Phys.* **1993**, 98, 5648.

[6] C. Lee, W. T. Yang, R. G. Parr, *Phys. Rev. B.* **1988**, 37, 785.

[7] *Gaussian 03,* Revision B.05; Gaussian, Inc., Wallingford CT, 2004.